ISSN 1674-1056
http://cpb.iphy.ac.cn
http://iopscience.iop.org/cpb
中国物理 B
Chinese Physics
中国物理
Chinese Physics B

Elastocaloric effect and mechanical behavior for NiTi shape memory alloys

Min Zhou(周敏), Yu-Shuang Li(李玉霜), Chen Zhang(张晨), Lai-Feng Li(李来风)

Citation: Chin. Phys. B . 2018, 27(10): 106501. **doi:** 10.1088/1674-1056/27/10/106501

Journal homepage: http://cpb.iphy.ac.cn; http://iopscience.iop.org/cpb

What follows is a list of articles you may be interested in

Large elastocaloric effect in Ti-Ni shape memory alloy below austenite finish temperature

Xiao-Hua Luo(罗小华), Wei-Jun Ren(任卫军), Wei Jin(金伟), Zhi-Dong Zhang(张志东)

Chin. Phys. B . 2017, 26(3): 036501. **doi:** 10.1088/1674-1056/26/3/036501

Response of thermal source in a transversely isotropic thermoelastic half-space with mass diffusion by finite element method

Ibrahim A. Abbas, Rajneesh Kumar, Vijay Chawla

Chin. Phys. B . 2012, 21(8): 084601. **doi:** 10.1088/1674-1056/21/8/084601

Generalized thermoelsticity of the thermal shock problem in an isotropic hollow cylinder and temperature dependent elastic moduli

Ibrahim A. Abbas, Mohamed I. A. Othman

Chin. Phys. B . 2012, 21(1): 014601. **doi:** 10.1088/1674-1056/21/1/014601

Elastocaloric effect and mechanical behavior for NiTi shape memory alloys*

Min Zhou(周敏)[1,†], Yu-Shuang Li(李玉霜)[2], Chen Zhang(张晨)[2], and Lai-Feng Li(李来风)[1,‡]

[1] Key Laboratory of Cryogenics, Technical Institute of Physics and Chemistry, Chinese Academy of Sciences, Beijing 100190, China
[2] School of Materials Science and Engineering, Beihang University, Beijing 100191, China

(Received 18 April 2018; revised manuscript received 11 June 2018; published online 10 September 2018)

The NiTi shape memory alloy exhibits excellent superelastic property and elastocaloric effect. The large temperature change (ΔT) value of 30 K upon loading and −19 K upon unloading are obtained at room temperature, which are higher than those of the other NiTi-based materials and among the highest values reported in the elastocaloric materials. The asymmetry of the measured ΔT values between the loading and unloading process is ascribed to the friction dissipation. The large temperature change originates from the large entropy change during the stress-induced martensite transformation (MT) and the reverse MT. A large coefficient-of-performance of the material is obtained to be 11.7 at $\varepsilon = 1\%$, which decreases with increasing the applied strain. These results are very attractive in the present solid-state cooling, which potentially could replace the vapor compression refrigeration technologies.

Keywords: elastocaloric effect, shape memory alloy, martensitic transformation, entropy change

PACS: 65.40.gd, 46.25.Hf, 62.20.fg **DOI:** 10.1088/1674-1056/27/10/106501

1. Introduction

Due to the large latent heat associated with the martensitic phase transformation, shape memory alloys are interesting candidates for solid state refrigeration.[1] Compared with the magnetocaloric[2–4] and electrocaloric cooling,[5,6] the elastocaloric cooling (whose caloric effect is driven by the uniaxial stress)[7–11] and barocaloric cooling (whose caloric effect is driven by the hydrostatic pressure)[12,13] have attracted much more attention in recent years. A giant barocaloric effect has been reported in the NiMnIn magnetic shape memory alloy in the past several years,[12] which was comparable to the magnetocaloric effect. What is more, the elastocaloric cooling technique has been assessed as being the most promising non-vapor compression mechanical refrigeration system because of its high coefficient of performance (COP) and moderate cost by the US Department of Energy[14] and opened the way to solid-state refrigeration.

Elastocaloric cooling is based on the diffusionless first order phase transformation of the shape memory alloy. The stress-induced martensite transformation leads to the heating of the material. After releasing the stress, the temperature of the material decreases due to the reverse martensite transformation. So, the elastocaloric effect can be regarded as the entropy change under isothermal condition ($\Delta S_{\rm iso}$) and temperature change under adiabatic condition ($\Delta T_{\rm adi}$) when a mechanical stress is used or released in a given material.[9] The COP is an important parameter of cooling technology, which describes the energy conversion efficiency at the operating temperature. For the convenience of estimation, the COP at a material level $\rm COP_{mater}$ ($= Q/W$) (here, $\rm COP_{mater}$ stands for coefficient-of-performance of the material) is calculated on the assumption that the material undergoes a specific cooling cycle with an ideal system configuration with full recoverable unloading energy and no auxiliary power consumption,[11,15,16] where Q is the cooling power and W is the input work. Besides, refrigeration capacity (RC), hysteresis, and the working temperature window are also noteworthy. The RC represents the amount of heat that can be transferred between the cold and hot sink in a thermodynamic cycle. It could be estimated according to the following relation[17]

$$RC = \int_{T_{\rm cold}}^{T_{\rm hot}} \Delta S_\sigma \, {\rm d}T, \tag{1}$$

where ΔS_σ is the stress-induced entropy change based on the Clausius–Clapeyron equation. $T_{\rm cold}$ and $T_{\rm hot}$ are the lower and upper temperature at full width half maximum of the ΔS_σ–T curve. The hysteresis originates from the energy dissipation in the form of frictional work and plastic accommodation, which is the intrinsic feature of the first-order phase transformation for the shape memory alloy. So it is adverse to the performance of the elastocaloric cooling. A wide working temperature window is imperative for practical elastocaloric cooling applications.

*Project supported by the Science Fund from the Key Laboratory of Cryogenics, Technical Institute of Physics and Chemistry, Chinese Academy of Sciences (TIPC, CAS) (Grant Nos. CRYOQN201501 and CRYO201218) and the National Natural Science Foundation of China (Grant Nos. 51577185, 51377156, and 51408586).

†Corresponding author. E-mail: mzhou@mail.ipc.ac.cn
‡Corresponding author. E-mail: laifengli@mail.ipc.ac.cn

© 2018 Chinese Physical Society and IOP Publishing Ltd

Compared with other shape memory alloys (FePd,[17] CuZnAl,[18,19] NiFe- and NiMn-based SMAs[11,12,20–25]), the NiTi-based shape memory alloys[7,10,15,26,27] show wonderful potential due to their good elastocaloric effect. In poly-crystalline NiTi wires, Cui *et al.* reported a large temperature change (ΔT) value of 25.5 K upon loading and 17 K upon unloading for the tension cycle. The obtained $\mathrm{COP_{mater}}$ values are 3.7 for the tension cycle and 11.8 for the compression cycle, respectively.[15] Large temperature changes of 21 K upon loading and −19 K upon unloading (at 342 K) were also reported in the loading-unloading trained NiTi alloy with an applied strain of 6%. Such high temperature changes contribute to the large entropy change (35.1 J/kg·K for loading and 33.9 J/kg·K for unloading process estimated by using the Clausius–Clapeyron equation).[28] Pataky *et al.*[23] and Wu *et al.*[29] then reported the elastocaloric effect of the NiTi single crystals. In Pataky *et al.*'s work, the temperature drops of 14.2 K and 13.3 K were observed in the [148] orientation and in the [112] orientation, respectively.[23] In Wu *et al.*'s work, a higher temperature drop was obtained to be 18.2 K in the [148] orientation.[29] Although the temperature changes of these NiTi single crystals were not higher than the above values of poly-crystal NiTi wires, the estimated entropy changes (maximum ΔS value of 69.64 J/kg·K in [148] orientation) of these NiTi single crystals were much higher than those of the poly-crystal NiTi wires. It is worth noting that the above stress-induced entropy changes each were calculated by the Clausius–Clapeyron relationship $\Delta S_\sigma \approx \nu_0 \Delta\varepsilon \, \mathrm{d}\sigma_\mathrm{t}/\mathrm{d}T$.[1] For the NiTi single crystals, the transformation strain $\Delta\varepsilon$ in the above equation was estimated using lattice deformation theory (LDT),[23,29] which may be higher than that obtained by the measured stress–strain curves. Besides, the elastocaloric effect of the NiTi (Cu) films was also reported.[10,26,30]

Because the great majority of applications require a large quantity of materials, it would therefore be desirable to study bulk elastocaloric materials. Here in this paper, we study the elastocaloric effect of the poly-crystalline NiTi bulks. Some key parameters (ΔT_adi, ΔS_iso, $\mathrm{COP_{mater}}$) of the elastocaloric effect are also estimated and discussed in a temperature change of 35 K (286 K–321 K), which is required for almost all practical solid-state cooling applications. The loading-unloading cycles of up to 1000 times are tested under a large strain level of 7%. The present poly-crystalline NiTi SMA exhibits an excellent elastocaloric effect, showing potential prospects in the solid-state refrigeration (or heat-pump) technologies.

2. Experimental methods

The starting materials were the poly-crystalline NiTi shape memory alloys ($\mathrm{Ni_{49.8}Ti_{50.2}}$). The diameters of the tensile testing samples were all 2 mm. They were annealed above the austenite finish temperature ($A_\mathrm{f} = 283$ K). The gauge length of the specimen between the two grips was 60 mm. The uniaxial tensile tests were conducted on a testing machine (20KN, SUNS). The material testing system was equipped with a cryogenic furnace. The stress–strain curves at different temperatures were recorded at a low strain rate of 1×10^{-4} s^{-1} to ensure the isothermal condition. For the elastocaloric cooling measurement, the sample was loaded at a much higher strain rate of 5×10^{3} s^{-1} (the maximum loading/unloading rate of the testing machine in the strain control mode) to approximately approach to the adiabatic condition, and then held for several minutes to make sure that the specimen temperature returned back to the environmental temperature. Then, the sample was unloaded quickly. The temperature changes in the loading, holding, and unloading process were monitored by a platinum resistance thermometer attached at the middle position of the sample. To improve thermal contact, the platinum resistance thermometer was attached by using silver paint and then was firmly kept in place by means of Teflon tape. The output of the platinum resistance thermometer was read by the Keithley-2000 multimeter at a frequency of 2 Hz. The strain was measured by an electronic extensometer (YYU-10/50, Central Iron and Steel Research Institute at room temperature, and 3542-025M-050-LT, Epsilon at cryogenic temperature). It is worth noting that the quicker unloading rate did not result in a larger temperature drop in our previous work,[31] so the unloading rate of 5×10^{3} s^{-1} was regarded as a reasonable value in this paper.

3. Results and discussion

3.1. Mechanical behaviors

Figure 1 (a) shows the stress–strain curves of the NiTi alloys with an applied strain of 7% at various temperatures. The NiTi alloys are tensile tested at approximately the isothermal hysteresis loop area (with a low strain rate of 1×10^{-4} s^{-1}). In the present case, the stress linearly increases with strain at low strain level ($\varepsilon = 1\%$) increasing, corresponding to the elastic response of the austenite phase. When the critical stress (σ_t) for stress-induced martensitic transformation is reached, a large transformation strain ($\Delta\varepsilon$) occurs at almost constant stress over the transformation plateau (the determination method of σ_t and $\Delta\varepsilon$ will be shown in Fig. 4(a)). Then the produced martensite phase is elastically deformed. After stress is released, the total strain can be fully recovered, indicating complete superelastic deformation in NiTi alloy. However, a little residual strain is observed at 313 K and 321 K, separately, which can be attributed to the dislocations generated by the stress-induced martensite transformation and remnant martensite stabilized by the dislocation strain field at higher temperatures. It is worth noting that the flat "plateau" appears in the loading and unloading processes of the stress-

strain curves, typically indicating the positive/reverse stress-induced MT. The "plateau" gradually moves to the higher stress with increasing temperature. As shown in Fig. 1(b), the critical transformation stress (σ_t) linearly increases with a slope of $d\sigma_t/dT = 8.194$ MPa·K^{-1} in the loading and 6.433 MPa·K^{-1} in the unloading process, separately. Figure 1(c) shows the variation of isothermal hysteresis loop area for loading-unloading cycles. It is worth noting that the NiTi binary alloy shows three phases (B2, R, and B19') based on the phase composition diagram, where the R phase is an intermediate transitional phase.[32] The stress-induced martensite transformation (A–M) undergoes the B2-R–B19 phase change process, while the reverse phase transformation (M–A) from B19' back to B2 is a single step process. The intrinsic two-step phase transformation and asymmetric phase transformation path on the phase diagram determine that the NiTi shape memory alloy has hysteresis during the phase transformation.[33] Like the behavior of the critical stress, the hysteresis loop area increases with temperature increasing. Both of them show that more input work is needed to induce the martensite transformation at higher temperature. It is worth noting that the hysteresis loop area turns to decrease at 321 K, which may be related to the insufficient phase transformation for the applied strain of 7% at higher temperature. Based on the stress-strain curves in Fig. 1(a), the Young's modulus is evaluated and shown in Fig. 1(d). The Young modulus is strongly temperature dependent and decreases with temperature decreasing, showing the softening of the trend towards the transition temperature ($A_f = 283$ K). It is reported that the Young moduli of both the martensite phase and austenite phase are temperature dependent and softened toward the transition temperatures for NiTi shape memory alloys. This is attributed to the shear phonon softening of the austenite phase and martensite phase in the vicinity of the transition temperature.[34–36] Quantitatively, the austenite phase of this NiTi alloy exhibits the softening (approximately 0.94 GPa·K^{-1}) with temperature decreasing.

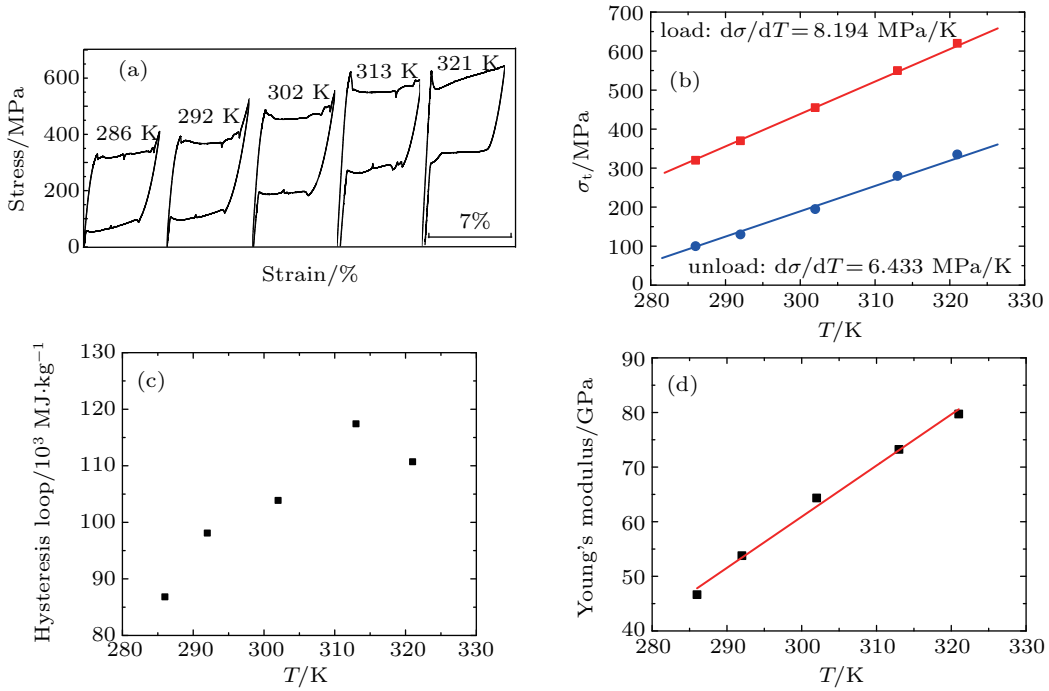


Fig. 1. (color online) (a) Isothermal stress–strain curves of NiTi alloys with applied strain of 7% at different temperatures. (b) Curves of critical stress of stress-induced MT and reverse MT versus temperature. (c) Isothermal hysteresis loop area of the above isothermal stress–strain curves at different temperatures. (d) Young's moduli of NiTi alloys at different temperatures.

3.2. Elastocaloric properties

Figure 2(a) shows the isothermal stress–strain curves (with a low strain rate of 1×10^{-4} s^{-1}) for different strain levels of 1%–7% at 291 K. The critical stress (σ_t) is reached at an applied strain of about 1%. Then the transformation plateau extends with increasing the applied strain. When the applied strain reaches to 7%, the stress-induced martensite transformation is completed and the produced martensite phase is elastically deformed. After the stress is released, the total strain could be fully recovered for all the applied strain levels, indicating an ideal superelastic deformation in NiTi alloy. The critical stress reaches to about 480 MPa with an applied maximum strain of 2% and then gradually decreases to 420 MPa when the applied maximum strain increases to 7%. The generation of internal stress with increasing strain is favorable for the formation of the stress-induced martensite phase, leading to the gradual degradation of the critical stress.[28] We also observe that the area of the stress hysteresis loop between the loading and unloading curve increases with strain increasing, showing that the fraction of martensite phase increases with

strain increasing.

In order to measure the adiabatic temperature change, an increased strain rate of 5×10^{-3} s^{-1} is used in the tensile test (Fig. 2(b)) and the temperature changes are shown in Fig. 2(c). The temperature change increases correspondingly with the strain increasing, which is attributed to the increase of the martensite volume fraction. When the applied strain increases to 7%, the temperature change ($\Delta T_{\text{loading}}$) reaches to its maximum value of 30 K upon loading due to the release of heat during the forward MT. During holding, the temperature change value recovers to the room temperature as a result of heat exchange between the sample and environment, and then decreases to -19 K upon unloading (ΔT_{unload}) due to the absorption of heat during reverse MT. Finally, the temperature change value recovers again to the room temperature during further holding due to the heat exchange.

The $\Delta T_{\text{loading}}$ value is not equal to the $\Delta T_{\text{unloading}}$ value at each strain level (1%–7%) (Fig. 2(c)), indicating the elastocaloric irreversibility ($\Delta T_{\text{irr}} = \Delta T_{\text{load}} \Delta T_{\text{unload}} \neq 0$) between the forward and reverse MTs. Analogous elastocaloric irreversibility was also reported in other NiTi alloys.[31,34] We also calculate the elastocaloric irreversibilities derived from the friction dissipation (ΔT_{fri}) by using the following equation[28]

$$\begin{aligned} \Delta T_{\text{fri}} &= (T\Delta S_{\text{fri}})/C_{\text{p}} = (TQ_{\text{hys}})/(C_{\text{p}}T) \\ &= \oint (\sigma \mathrm{d}\varepsilon)/(\rho C_{\text{p}}), \end{aligned} \tag{2}$$

where the density (ρ) is 6.71 g·cm^{-3}, and the specific heat (C_{p}) is measured to be 0.432 J·g^{-1}·K^{-1} for the NiTi alloy. The Q_{hys} value is the stress hysteresis area of the isothermal test. The irreversible entropy change (ΔS_{fri}) is obtained from the stress hysteresis area of the stress–strain curve under the isothermal condition (Fig. 2(a)) since the stress hysteresis under the adiabatic condition additionally includes the thermodynamic work needed to perform the cooling cycle with self-heating and self-cooling of the material.[28] The obtained ΔT_{fri} values are plotted in Fig. 2(d). They are consistent with the measured ΔT_{irr} values, which confirms that the friction dissipation contributes to the elastocaloric irreversibility.

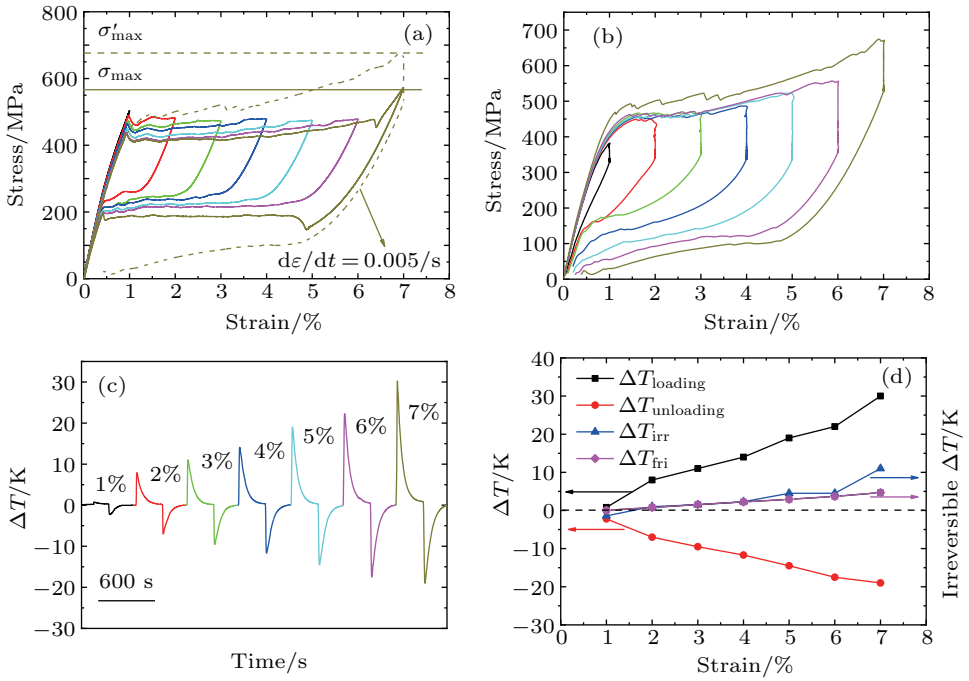


Fig. 2. (color online) (a) Stress–strain curves at different strain levels (ε = 1%–7%) under an approximately isothermal condition (low strain rate of 1×10^{-4} s^{-1}). (b) Stress–strain curves at different strain levels (ε = 1%–7%) under an approximately adiabatic condition (high strain rate of 5×10^{-3}/s) at room temperature. Higher strain rate leads to both higher critical stresses and larger stress hysteresis. (c) Corresponding ΔT-time profiles at different strain levels (ε = 1%–7%). (d) ΔT-strain profiles at different strain levels (ε = 1%–7%) in the loading and unloading process. All the above tensile tests are conducted at room temperature.

Figure 3 shows the measured temperature changes of NiTi alloys in a wider temperature range of 286 K–321 K, which is required for almost all practical solid-state cooling applications. Large temperature changes of 20 K$\sim$ 30 K upon loading and -13 K$\sim$ -19 K upon unloading are observed with an applied strain of 7% in the measured temperature range. The maximum temperature change ($\Delta T_{\max}$) values are 30 K upon loading and -19 K upon unloading at 291 K, respectively, which are even higher than the measured ΔT values of some other reported NiTi alloys (such as the poly-crystalline NiTi wires,[15,31] the trained poly-crystalline NiTi wires,[28] the NiTi single crystal,[23,29] and the NiTi thin film[30]).

Based on the Clausius–Clapeyron equation, the stress-induced entropy change (ΔS_σ) can be calculated from $\Delta S_\sigma \approx \Delta S_{\text{iso}} = -\nu_0 \Delta\varepsilon \, \mathrm{d}\sigma_{\text{t}}/\mathrm{d}T$,[1] where T is the ambient temperature in Kelvin, C_{p} is the specific heat (432 J·kg^{-1}·K^{-1}), ν_0 is the

specific volume of 1.48×10^{-4} m^3 kg^{-1}), $\Delta\varepsilon$ is the transformation strain, and $\mathrm{d}\sigma_t/\mathrm{d}T$ is the critical transformation stress dependence on temperature (shown in Fig. 1(b)). As a result, large ΔS_σ values of -60.6 J·kg^{-1}·K^{-1} ~ -75.8 J·kg^{-1}·K^{-1} for loading and 45.7 J·kg^{-1}·K^{-1} $\sim$ 49.5 J·kg^{-1}·K^{-1} for unloading process are obtained in the measured temperature range of 286 K–321 K (Fig. 4(b)), respectively, which are higher than those of some other poly-crystalline NiTi alloys.[28,31] So the above high temperature changes can be attributed to these large entropy changes. In the NiTi single crystals, a larger theoretical ΔS_σ value of 69.64 J·kg^1·K^{-1} is reported in the [148] orientation, in which the transformation strain ($\Delta\varepsilon_{cal}$) is calculated by using the lattice deformation theory (LDT).[23] The $\Delta\varepsilon_{cal}$ value is the potential attainable transformation strain. So the measured temperature drop (-14 K) is not higher than our results (shown in Fig. 3).

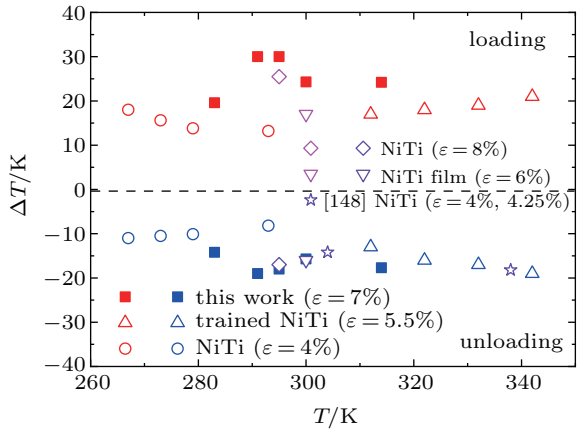


Fig. 3. (color online) Measured temperature changes of NiTi alloys in the loading and unloading process with an applied strain of 7%. The open triangles correspond to the measured ΔT values of trained poly-crystalline NiTi alloy with applied strain of 5.5%.[28] Open cycles correspond to the measured ΔT values of the poly-crystalline $Ni_{50.8}Ti_{49.2}$ alloy with applied strain of 4%.[31] Open diamonds correspond to measured ΔT values of poly-crystalline NiTi wires with applied strain of 8%.[15] The open down-triangles correspond to measured ΔT values of NiTi films with applied strain of 6%.[30] Open stars correspond to the measured ΔT values in [148] orientation of NiTi single crystals with applied strains of 4%[29] and 4.25%.[23]

As mentioned above, the COP_{mater} is expressed as the ratio of cooling power (Q) to input work (W) ($COP_{mater} = Q/W = \Delta T_{adi} C_p \rho / W$),[11,15] where ΔT_{adi} is the theoretical temperature change under the adiabatic condition, which is a potentially attainable value. In the following, the COP_{mater} value is approximately estimated ($COP_{mater} \approx \Delta T_{mea} C_p \rho / W$) by using the measured temperature change (ΔT_{mea}). Based on the adiabatic stress–strain curves at room temperature (Fig. 2(b)), the input work (W) in the unloading process is calculated by integrating the area enclosed by the loading and the unloading curve.[11,15] With a density of 6710 kg·m^{-3} and heat capacity of 432 J·kg^{-1}·K^{-1}, the COP_{mater} value is estimated at different strain levels (ε = 1%–7%) and shown in Fig. 5. The COP_{mater} values show an inverse dependency on the applied strain level. When the applied strain level is ε = 1%, the obtained COP_{mater} value is 11.7. With increasing the applied strain level, the COP_{mater} values decrease. Smaller strain amplitudes should be used to increase the COP_{mater} values. Analogous results were reported in NiFeGa magnetic shape memory alloy.[35] However, larger strain should be loaded up to obtain high temperature change. So, a moderate strain level will be adopted in the actual cooling application.

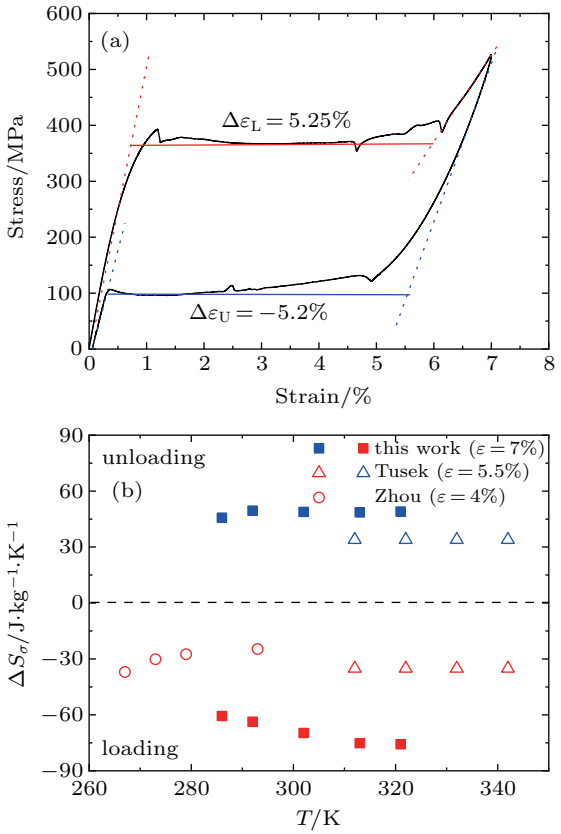


Fig. 4. (color online) (a) Transformation strain ($\Delta\varepsilon$) values during stress-induced MT and the reverse MT at room temperature. (b) Stress-induced entropy change (ΔS_σ) values of NiTi alloys. Open cycles correspond to the data of the poly-crystalline $Ni_{50.8}Ti_{49.2}$ alloy.[31] Open triangles correspond to the data of trained poly-crystalline NiTi alloy.[28]

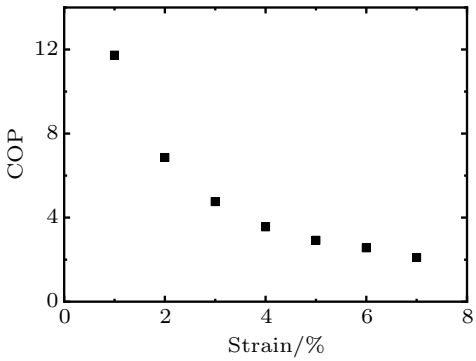


Fig. 5. The COP_{mater} values of the NiTi alloys at different strain levels (ε = 1%–7%) in the unloading process.

The tensile cycling test is performed 1000 times with a high strain rate (5×10^{-3} s^{-1}) at 300 K. The ΔT_{max} values of the first cycle are 29 K upon loading and -17 K upon unloading, respectively, under a large strain level of 7% (Figs. 6(a)

and 6(b)), which is consistent with the above results of other samples. With increasing the cycle numbers, the ΔT_{max} value gradually decreases and then gradually stabilizes at 23 K upon loading and −6 K upon unloading when the cycle number is over 200. The decrease of ΔT_{max} with increasing cycle number is also observed in some other elastocaloric materials,[11,31] which is attributed to the accumulation of dislocations with increasing cycles. In Figs. 6(c) and 6(d), we observe the decrease of the critical stress of martensitic transformation, the area of hysteresis loop and the transformation strain, which confirms the accumulation of defects with increasing cycles. The initially formed dislocations and remnant martensite, in turn, suppress the dislocation generation in the subsequent long-term cycles, which leads to the stabilization of the temperature changes.[28,29,36] However, it is still not enough to evaluate the elastocaloric stability (long-term stress cycles on the order of 10^6 would be needed). In the next work, the microstructural modification by doping (Cu, Co, etc.) or incorporating the ductile second phase into grain boundaries, and mechanically training pretreatment of elastocaloric materials are expected to enhance mechanical and elastocaloric stability. Moreover, the compression, instead of tension, will restrain the fatigue crack growth and lead to a longer life span.

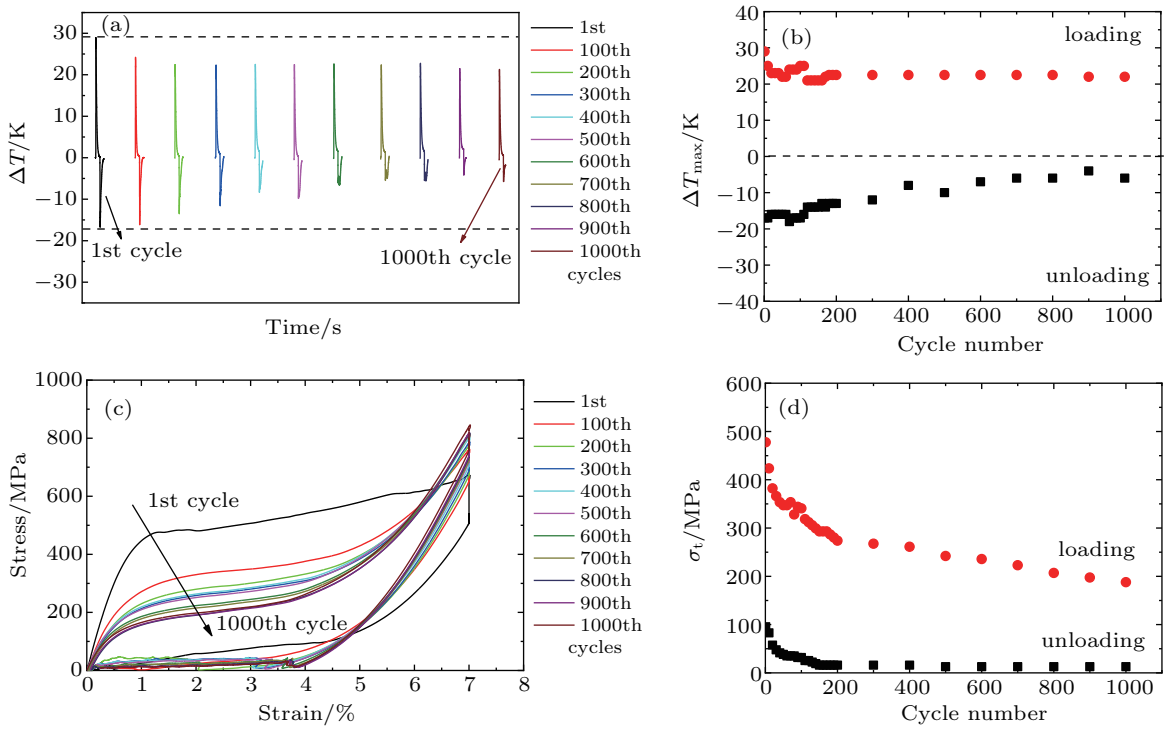


Fig. 6. (color online) (a) Representative temperature variations of NiTi alloy (with an interval of 100 times, 1st, 100th, 200th, …, and 1000th cycle) during tensile cycling tests with a strain rate of 5×10^{-3} s^{-1} at room temperature. (b) Measured maximum temperature change ΔT_{max} as a function of the cycle number. (c) Representative stress–strain curves of NiTi alloys (with an interval of 100 times, the 1st, 100th, 200th, …, and the 1000th cycle). (d) Critical stress of martensitic transformation as a function of cycle number.

4. Conclusions

In summary, the present NiTi alloys not only exhibit an excellent shape memory effect and superelasticity but also show a giant elastocaloric effect. Large temperature changes of 19 K∼ 30 K upon loading and −13 K∼ −19 K upon unloading were measured, respectively, in a temperature range of 35 K (286 K–321 K). The maximum ΔT values (ΔT_{max}) of 30 K upon loading and −19 K upon unloading are measured at room temperature, respectively, which are higher than those of the other NiTi-based elastocaloric materials and among the highest values of the elastocaloric materials. The asymmetry of the measured ΔT values between loading and unloading depends on the applied strain level and is ascribed to the friction dissipation. The large temperature changes mainly originate from the large entropy change (-60.6 J·kg^{-1}·K^{-1} ∼ -75.8 J·kg^{-1}·K^{-1} for loading and 45.7 J·kg^{-1}·K^{-1} ∼ 49.5 J·kg^{-1}·K^{-1} for unloading process) during the stress-induced MT and the reverse MT. The ΔT_{max} values decrease in the first 200 mechanical cycles and then gradually stabilize at 23 K upon loading and −6 K upon unloading with tensile cycle number increasing up to 1000 cycles, showing the cyclic stability of the elastocaloric effect. The accumulation of defects is supposed to contribute to the decrease of ΔT_{max} values. A COP_{mater} of 11.7 is obtained at $\varepsilon = 1\%$, which decreases with applied strain increasing. The present NiTi alloy exhibits larger temperature change (ΔT) and entropy change (ΔS_σ) than the reported NiTi elastocaloric materials, and shows strong competitive ability in the solid-state refrigeration (or heat-pump) technologies.

References

[1] Bonnot E, Romero R, Manosa L, Vives E and Planes A 2008 *Phys. Rev. Lett.* **100** 125901

[2] Gschneidner K A, Pecharsky V K and Tsokol A O 2005 *Rep. Prog. Phys.* **68** 1479

[3] Planes A, Manosa L and Acet M 2009 *J. Phys.: Conden. Matter* **21** 233201

[4] Smith A, Bahl C R H, Bjork R, Engelbrecht K, Nielsen K K and Pryds N 2012 *Adv. Energy Mater.* **2** 1288

[5] Mischenko A S, Zhang Q, Scott J F, Whatmore R W and Mathur N D 2006 *Science* **311** 1270

[6] Moya X, Stern-Taulats E, Crossley S, Gonzalez-Alonso D, Kar-Narayan S, Planes A, Manosa L and Mathur N D 2013 *Adv. Mater.* **25** 1360

[7] Moya X, Kar-Narayan S and Mathur N D 2014 *Nat. Mater.* **13** 439

[8] Crossley S, Mathur N D and Moya X 2015 *AIP Adv.* **5** 067153

[9] Manosa L, Planes A and Acet M 2013 *J. Mater. Chem. A* **1** 4925

[10] Bechtold C, Chluba C, De Miranda R L and Quandt E 2012 *Appl. Phys. Lett.* **101** 091903

[11] Xiao F, Jin M, Liu J and Jin X 2015 *Acta Mater.* **96** 292

[12] Manosa L, Gonzalez-Alonso D, Planes A, Bonnot E, Barrio M, Tamarit J L, Aksoy S and Acet M 2010 *Nat. Mater.* **9** 478

[13] Yuce S, Barrio M, Emre B, Stern-Taulats E, Planes A, Tamarit J L, Mudryk Y, Gschneidner K A Jr Pecharsky V K and Manosa L 2012 *Appl. Phys. Lett.* **101** 071906

[14] Goetzler W, Zogg R, Young J and Johnson C 2014 *US Department of Energy*

[15] Cui J, Wu Y, Muehlbauer J, Hwang Y, Radermacher R, Fackler S, Wuttig M and Takeuchi I 2012 *Appl. Phys. Lett.* **101** 073904

[16] Lu B and Liu J 2017 *Sci. Rep.* **7** 2084

[17] Xiao F, Fukuda T and Kakeshita T 2013 *Appl. Phys. Lett.* **102** 161914

[18] Manosa L, Jarque-Farnos S, Vives E and Planes A 2013 *Appl. Phys. Lett.* **103** 211904

[19] Vives E, Burrows S, Edwards R S, Dixon S, Manosa L, Planes A and Romero R 2011 *Appl. Phys. Lett.* **98** 011902

[20] Yang Z, Cong D Y, Huang L, Nie Z H, Sun X M, Zhang Q H and Wang Y D 2016 *Mater. & Design* **92** 932

[21] Sun W, Liu J, Lu B, Li Y and Yan A 2016 *Scr. Mater.* **114** 1

[22] Huang Y J, Hu Q D, Bruno N M, Chen J H, Karaman I, Ross J H Jr and Li J G 2015 *Scr. Mater.* **105** 42

[23] Pataky G J, Ertekin E and Sehitoglu H 2015 *Acta Mater.* **96** 420

[24] Wang D H, Han Z D, Xuan H C, Ma S C, Chen S Y, Zhang C L and Du Y W 2013 *Chin. Phys. B* **22** 077506

[25] He W, Huang H, Liu Z and Ma X 2018 *Chin. Phys. B* **27** 016201

[26] Ossmer H, Chluba C, Gueltig M, Quandt E and Kohl M 2015 *Shape Memory Superelasticity* **1** 142

[27] Luo X H, Ren W J, Jin W and Zhang Z D 2017 *Chin. Phys. B* **26** 036501

[28] Tusek J, Engelbrecht K, Mikkelsen L P and Pryds N 2015 *J. Appl. Phys.* **117** 124901

[29] Wu Y, Ertekin E and Sehitoglu H 2017 *Acta Mater.* **135** 158

[30] Ossmer H, Lambrecht F, Gueltig M, Chluba C, Quandt E and Kohl M 2014 *Acta Mater.* **81** 9

[31] Zhou M, Li Y, Zhang C, Li S, Wu E, Li W and Li L 2018 *J. Phys. D: Appl. Phys.* **51** 135303

[32] Egorushkin V E, Kulmentyev A I and Flat A Y 1987 *J. Phys. F: Metal Phys.* **17** 289

[33] Qian S, Geng Y, Wang Y, Ling J, Hwang Y, Radermacher R, Takeuchi I and Cui J 2016 *Int. J. Refrigeration-Rev. Int. Du Froid* **64** 1

[34] Zhao D, Liu J, Feng Y, Sun W and Yan A 2017 *Appl. Phys. Lett.* **110** 021906

[35] Li Y, Zhao D and Liu J 2016 *Sci. Rep.* **6** 25500

[36] Yang Z, Cong D Y, Sun X M, Nie Z H and Wang Y D 2017 *Acta Mater.* **127** 33